Metal particle induced spacer surface charging phenomena in direct current gas-insulated transmission lines

Metal particle induced spacer surface charging phenomena in DC GIL

Yunqi Xing[1], Xinbo Sun[1], Yang Yang[2,a)], Giovanni Mazzanti[3], Davide Fabiani[3], Jinliang He[2] and Chuanyang Li[2, b),c)]

[1] State Key Laboratory of Reliability and Intelligence of Electrical Equipment, Hebei University of Technology, Tianjin,300131, China
[2] State Key Laboratory of Power Systems, Department of Electrical Engineering, Tsinghua University, Beijing, 100084, China
[3] Dept. Electrical, Electronic and Information Engineering, University of Bologna, Viale Risorgimento 2, Bologna 40136, Italy

[a)] Now with Simpson Querrey Institute, Northwestern University, Evanston, IL 60208, United States
[b)] Now with University of Connecticut, Storrs, CT 06269, United States
[c)] Author to whom correspondence should be addressed: lichuanyangsuper@163.com

Abstract

The interpretation of the surface charge pattern of spacers in gas-insulated transmission lines (GIL) is a crucial and important research topic, which requires a comprehensive understanding of charge behaviors at physical interfaces. Here, we report a surface charging phenomenon of spacers in presence of metal particles inside the direct current (DC) GIL. The charging of spherical metal particle on the spacer surface appears as dotted discontinuously distributed charge spots which are due to the charge injection from the induced charge of the metal particle and gas ionization over the metal particle surface. Concentrically distributed bipolar charge patterns are seen to build up, which are due to the surface trapping of charges from gas ionization at the end tip of the acicular metal particle. The lateral type of ionization obeys the law of dielectric barrier discharge of the needle-plate electrode at an intense DC electric field, which may bring significant influence on the safety of the spacer. The study in this letter provides direct evidence demonstrating the surface charge patterns of spacers in the presence of metal particles, which serves as an important basis in the design of DC GIL.

Keywords: surface charge, DC GIL, dust figure, metal particle

1. Introduction

Gas-insulated transmission lines (GIL) have great potential in the construction of future ultra-high-voltage AC/DC power transmission, urban substations, and offshore converter stations[1-3]. The unavoidable metal particle movement inside the GIL affects the surface charge accumulation of the spacer, which potentially triggers undetermined spacer surface flashover[4-7].

The surface charging behavior of the spacer follows the field-dependent theory[8]. The charges may be (i) homo-polar, which are injected from the electrode and reduce the flashover voltage in a manner of shortening the so-called "analogous ineffective region"[9]. (ii) hetero-polar coming from the gas ionization, which significantly reduces the flashover voltage depending on its charge density and position[10], (iii) homo-polar charge due to ionization of partial discharges affects/decreases the flashover voltage which is determined by the charge location, distribution, and density[11-15]. The presence of the metal particles distorts the local electric field and cause local ionization, providing a source of space charge carriers in the gas phase, which may serve as a source to increase the amount of spacer surface charges[10]. However, so far, we know very few about the metal particle movement over the spacer surface and there is a lack of theoretical and experimental research results on

how the metal particles may be the source of surface charge which accumulates on the spacer at DC voltage[16,17].

In this study, we successfully presented the surface charging behavior of spacers in the presence of metal particles by using the dust figure technique, and the surface charge accumulation properties of spacers induced by metal particles were demonstrated. The work described in this letter serves as important evidence unfolding the charging phenomena of spacers by metal particles and provides a reference for further design of DC GIL.

2. Experimental descriptions

The model spacer was prepared employing an industrially used epoxy and micron-sized alumina using vacuum casting. The model spacer and the model GIL can refer to our previously published articles[8,10]. The experimental setup can be found in Fig. 1(a). Before the experiment, the surface of the sample was cleaned by using a grounded alcohol cloth and stored at room temperature for more than 24 h. The experiment was performed inside a chamber filled with 0.2 MPa SF_6, and this pressure value is a typical value of pressure used in DC GIL to avoid flashover of spacers in this model GIL during test. The voltage was increased with a boosting rate of 1 kV/s. The metal particles are made of aluminum, as shown in Fig. 1(b). The diameter of the spherical metal particle is 2 mm. The diameter and the length of the acicular metal particle are 0.2 mm and 10 mm, respectively. These shapes and sizes of the metal particles were chosen since they well represent the typical shapes and sizes of metal particles in DC GIL[18].

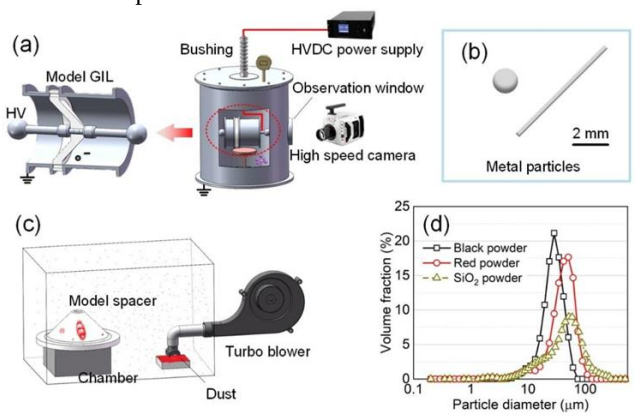

FIG. 1. Experimental setup and samples. (a) Schematic diagram of observation platform of metal particle movement experiment: (b) dimensions of metal particles size; (c) schematic diagram of the dust figure test platform; (d) dust powder diameter distribution.

During the experiment, the metal particles were placed at a horizontal distance of 0 mm and 10 mm from the bottom of the model spacer. A high-speed camera (Phantom v611) was used to observe the movement of the metal particles (acquisition rate = 500 fps, resolution = 1024 × 512 pixels, exposure time = 999.566 μs). After the test, the spacer was taken out and transferred to another PMMA chamber for dust figure treatment, as shown in Fig. 1(c). The dust powders used in this paper are red carbon powder with a negative charge, black carbon powder with a positive charge, and electrically neutral silicon oxide powder. The diameter distribution diagram of these powders is shown in Fig. 1(d).

3. Results

Fig. 2 shows the trajectory of metal particles. It is worth noting that, compared with the acicular metal particle, the spherical metal particle has a lower lifting voltage, and as the distance between the particle and the spacer increases from 0 mm to 10 mm, the lifting voltage rises from 46.1 kV to 50.7 kV. For the acicular particle, the lifting voltages are 31.9 kV and 38.0 kV with distances of 0 mm and 10 mm from the spacer.

As can be seen by the take-off trajectories of spherical particles in Fig. 2(a) and (b), once the lifting voltage of the spherical metal particle is reached, the particle accelerates towards the high-voltage conductor at a relatively slow initial speed along the radial direction of the cylinder. When the particle is close to the spacer, it rolls up along the surface of the spacer. When the particle is 10 mm away from the spacer, the particle first moves vertically upwards to get in touch with the surface of the spacer, then it rolls upward along the surface of the spacer until it collides with the high-voltage conductor. Subsequently, the particle hops back and forth between the center conductor and the metal shell at a higher speed and gradually moves away from the spacer. The detailed particle motion can be found in supplementary materials 1 and 2.

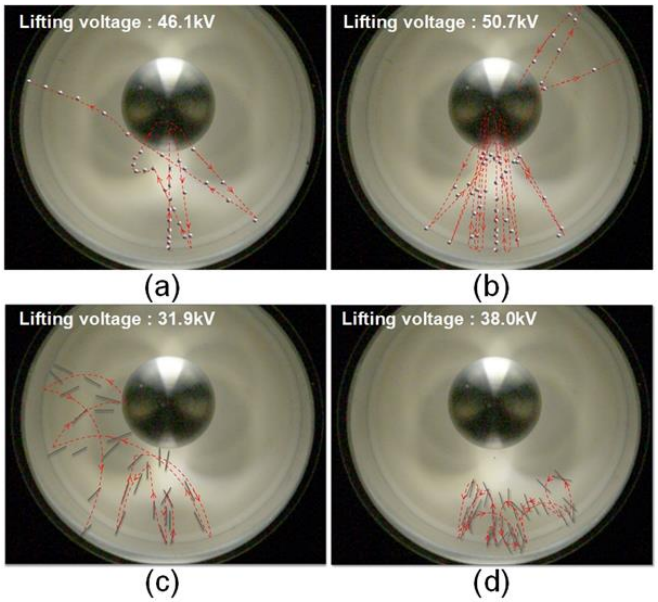

FIG. 2. The take-off trajectories of spherical (a, b) and acicular (c, d) metal particles with the distance from particle to spacer of 0 mm (a, c) and 10 mm and (b, d).

Fig. 2(c) and (d) show the take-off trajectories of acicular particles with a distance of 0 mm and 10 mm from the spacer, respectively. Compared with spherical metal particles, the trajectory of the acicular metal particle is more complicated. The particle motion includes rotation, tumbling, and up and down reciprocating motion. Once the lifting voltage is reached, one end of the acicular particle is lifted first and hit the spacer at a low speed. Accompanied by the high-speed reciprocating collision movement between the spacer and the metal shell, the particle rotates continuously and gradually moves away from the spacer until it flies out of the GIL model. Interestingly, when the acicular metal particle hits the spacer, there is a certain probability that it will be adsorbed on the surface of the spacer. The videos of particle motion can be found in supplementary materials 3 and 4.

Fig. 3 shows the surface dust pattern of the spacer treated by the dust figure method. When there were no metal particles (Fig. 3(a) - (c)), no local dust clusters were found on the spacer surface after applying 52 kV for 1 min, which represents that there would be no charge accumulation on the surface without metal particles up to this voltage level. When the spherical metal particle was 0 mm away from the spacer, concentrically distributed bipolar dotted dust patterns could be observed close to the high-voltage conductor, as shown in Fig. 3(d) - (f). When the spherical metal particle was 10 mm away from the spacer, as shown in Fig. 3(g) - (i), more dust patterns in the areas where the metal particle initially hit the spacer surface were observed. Additionally, more positive red carbon powders were found attached to the spacer surface near the HV conductor in Fig. 3(f) and (i).

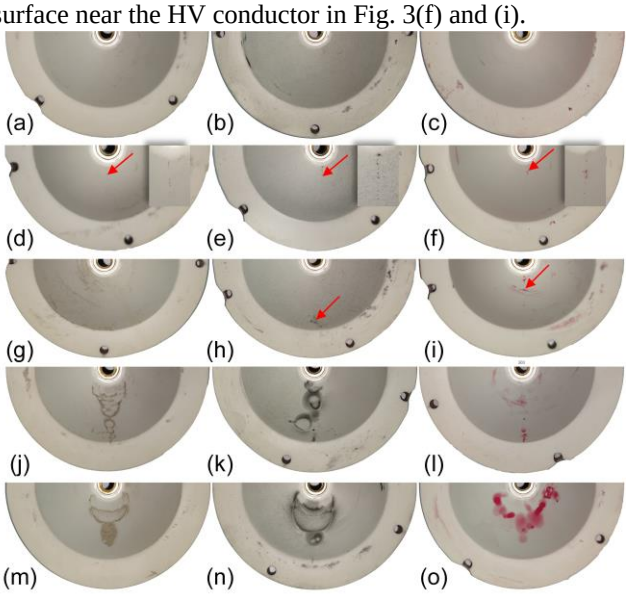

FIG. 3. The surface dust patterns of the spacer treated by the dust figure method using neutral, positive- and negative-polar powders, respectively. (a)-(c) 52 kV for 1 min with no metal particles nearby, (d)-(f) with a spherical particle close to the spacer, (g)-(i) with a spherical particle 10 mm from the spacer, (j)-(l) with an acicular particle close to the spacer, and (m)-(o) with an acicular particle 10 mm from the spacer. The dust figure of these four groups (a-c, d-f, g-i, j-l) refer to different numbers of experiment.

4. Discussion

The dust figure method has been verified effectively to reproduce the surface charge characteristics[19]. It should be considered that the hetero-polar powder is attracted by the spacer surface to reproduce the polarity and distribution characteristics of the surface charge, while the neutral powders are polarized under the electric field generated by the spacer surface charge and form an electric field gradient map on the surface of the spacer[8,10]. Based on the field-dependent theory, at a lower electric field[8], the convex surface of the spacer accumulates a small amount of homo-polar charges when there is no ionization from the gas phase, as is indicated by Fig. 3(a)-(c). As a result, metal particles close to the spacer have a lower lift-off voltage.

When the lift-off voltage is reached, a large amount of hetero-polar charges on the spherical particle surface is induced. These hetero-polar charges are injected into the spacer surface when the spherical particle touches the spacer, which supports the phenomenon of the black powders on the spacer surface as shown in Fig. 3(h). However, when the spherical particle is lifted to the nearby of the HV conductor, due to the sharp increase in the applied electric field strength, the field between the spherical particle and the spacer surface is distorted and gas ionization in between occurs, which introduces both hetero- and homo-polar surface charges. This assumption is verified by the distribution of red and black powders shown in Fig. 3(e), (f) and (i).

However, it is interesting to note that each time after the charge transfer from the spherical particle to the spacer surface, the surface charge on the spherical particles decreases, and it takes some time to re-accumulate enough charge until the next ionization. This is the reason why the charge spots we observe are dotted distributed rather than linearly distributed. Fig. 4 shows the relationship between the acceleration and velocity of metal particles at different surface positions. It can be seen that as the spherical metal particle moves closer to the HV conductor, the acceleration and the velocity have an increasing trend. However, some sharp decreases in the acceleration can be found in Fig. 4(c) marked as A, B, and C, which corresponding to the charged position presented by the colored powders shown in Fig. 4(a) and (b). This finding verifies the charge transfer during the movement of metal particles which causes the electric field force to drop, resulting in a sharp decrease in acceleration.

Rotation may be due to the horizontal force on the tip of the needle as the voltage gradually increases. This force may be due to the local inhomogeneity of the needle or to the contribution of the ionistic wind generated by the transverse corona. The specific principle still needs to be further verified.This explains why a stable stage exists before the particle touches the HV conductor. The plasma flow due to the ionization exerts a horizontal force on the particles, which is the reason why the particle rotates at a position

close to the grounded shell before being lifted to touch the HV conductor, as has been presented by Fig. 2(c) and (d) as well as the supplementary materials 3 and 4.

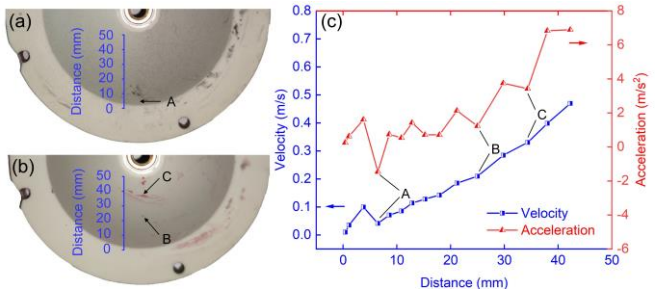

FIG. 4. The velocity and the acceleration of spherical metal particles at different positions along the spacer. (a) dust figures patterns, and (b) the corresponding velocity and acceleration.

When the acicular metal particle is closer to the bottom of the spacer after the lift-off voltage, the spacer surface can be charged due to the ionization, resulting in a charged region near the bottom of the spacer as shown in Fig. 3(j)-(l). However, when the metal particle is 10 mm away from the spacer, a relatively large-area charge accumulation pattern close to the HV conductor can be observed. This occurs because the extension of the plasma path leads to an increase in its radius, as shown in Fig. 3(m)-(o). It is interesting to emphasize that we found spots-like homo-polar charge accumulated near both electrodes, while hetero-polar charges appeared on the outer edge, as shown in Fig. 3(k), (l), (n), and (o). This physical phenomenon follows the law of dielectric barrier discharge of the needle-plate electrode at intense DC electric field, i.e., when the electric field was severely distorted, on the surface of the barrier dielectric, hetero-polar charges can be observed as presented in the center area of homo-polar charges[8,10]. The hetero-polar charges on the spacer surface introduced by the acicular metal particle decreases the electric field near the metal particle, which explains why higher voltage is required for the lift-off of the acicular metal particle far away from the spacer. However, the existence of hetero-polar surface charges may increase the possibility of spacer flashover, which brings significant influence on the safety of the spacer[10]. It should be emphasised that hetero-polar charges are seen with spherical particles in Fig. 3(h), however, those charges are injected charges when the spherical particle touches the spacer, which do not show a concentric circle with homo-polar charges in the outer ring and hetero-polar charges in the center.

5. Conclusion

A surface charging phenomenon of spacers in presence of metal particles at DC voltage is reported in this letter. It is found that the lift-off voltage of the acicular particle is significantly lower than that of the spherical particle. Due to the induction and ionization of the metal particle near the conductors, the charging of the spherical metal particle on the spacer surface appears as dotted discontinuously distributed charge spots. Ionization from the end of the acicular metal particle generates charge carriers which traps on the spacer surface, forming concentrically distributed bipolar surface charge patterns. The hetero-polar charges on the spacer surface introduced by the acicular metal particle may increase the possibility of spacer flashover, which brings significant influence on the safety of the spacer. However, the hetero-polar charges from spherical particles are injected charges when the spherical particle touches the spacer, which do not show a concentric circle with opposite charge polarity. This paper provides evidence demonstrating the surface charge patterns of spacers in the presence of metal particles, which serves as an important basis in the design of particle traps for DC GIL.

We agree that the possibility that charges on the spacer surface may be different before inside the SF_6 and after this spacer was taken out exists. However, we would say that to decrease the operation time can be helpful in mitigating the changing of charge distribution and density. This has been discussed by previous studies[20,21].

Additionally, due to the limitation of dust figure method, we have no access to the charge density but only the charge distribution and charge polarity. For epoxy based materials, due to reasonably low surface conductivity, the changing of such parameters would be smaller compared with the charge density[22-26].

See the supplementary materials for the detailed particles motion.

Acknowledgements

This work was supported by the Young Scientists Fund of the National Natural Science Foundation of China under NSFC Grant No. 51907047.

References

[1] G Mazzanti, G Stomeo and S Mancini 2016 *IEEE Electrical Insulation Magazine* **32** 18
[2] C Li, C Lin, B Zhang, Q Li, W Liu, J Hu and J He 2018 *IEEE Transactions on Dielectrics and Electrical Insulation* **25** 1152
[3] C Cooke 1982 *IEEE Transactions on Dielectrics and Electrical Insulation* **2** 172
[4] E Volpov 2004 *IEEE Transactions on Dielectrics and Electrical Insulation* **11** 949
[5] H Iwabuchi, S Matsuoka, A Kumada, K Hidaka, Y Hoshina, T Yasuoka and M Takei 2013 *IEEE Transactions on Dielectrics and Electrical Insulation* **20** 1895
[6] H Wang, J Xue, J Chen, J Deng, G Zhang and S Meng 2019 *AIP Advances* **9** 085212
[7] J Sun, L Sun, W Chen, Z Li, X Yan, X Yan and Y Xu 2019 *High Voltage* **4** 138
[8] C Li, C Lin, G Chen, Y Tou, Y Zhou, Q Li, B Zhan, Lin C, Chen G and J He 2019 *Applied Physics Letters* **114** 202904

[9] C Li, J Hu, C Lin and J He 2017 *Scientific Reports* **7** 3271
[10] C Li, Y Zhu, J Hu, Q Li, B Zhan and J He 2020 *Journal of Physics D Applied Physic*s **54** 015308
[11] J Xue, H Wang, J Chen, K Li, Y Liu, B Song, J Deng and G Zhang 2018 *Journal of Applied Physics* **124** 083302
[12] J Xue, Y Li, J Dong, J Chen, W Li, J Deng and G Zhang 2020 *Journal of Physics D: Applied Physics* **53** 155503
[13] A Winter and J Kindersberger 2001 *Elektrie* **10-12** 536
[14] A Winter and J Kindersberger 2002 *Annual Report Conference on Electrical Insulation and Dielectric Phenomena*
[15] S Kumara, S Alam, I R Hoque, Y V Serdyuk and S M Gubanski 2012 *IEEE Transactions on Dielectrics and Electrical Insulation* **19** 1084
[16] T Magier, M Tenzer and H Koch 2018 *IEEE Transactions on Power Delivery* **33** 440
[17] F Hammer and A Kuchler 1992 *IEEE Transactions on Dielectrics and Electrical Insulation* **27** 601
[18] K Park, S G Goo, J Y Yoon, W H Kye, T Y Kwon, S Rim, C M Kim and Y J Park 2003 *Applied Physics Letters* **83** 195
[19] C Li, Q Zhi, J Sun, Z Li, S Song, Y Zhu, G Chen and Z Lei 2021 *IEEE Transactions on Dielectrics and Electrical Insulation* DOI: 10.1109/TDEI.2021.009432
[20] J Xue, J Chen, J Dong, J Deng and G Zhang 2020 *Nanotechnology* **31** 364002
[21] J Xue, J Chen, J Dong, G Sun, J Deng, G Zhang 2020 *International Journal of Electrical Power & Energy Systems* **120** 105979
[22] J Kindersberger and C Lederle 2008 *IEEE Transactions on Dielectrics and Electrical Insulation* **15** 941
[23] J Kindersberger and C Lederle 2008 *IEEE Transactions on Dielectrics and Electrical Insulation* **15** 949
[24] B Zhang and G Zhang 2017 *Journal of Applied Physics* **121** 105105
[25] B Du and J Li 2016 IEEE Transactions on Dielectrics and Electrical Insulation **23** 1190
[26] B Du, H Liang, J Li and C Zhang 2018 IEEE Transactions on Dielectrics and Electrical Insulation **25** 631